JOURNAL OF AIRCRAFT
Vol. 37, No. 5, September–October 2000

Experimental Demonstration of the Influence of Wing Couplings on Whirl–Flutter Instability

Omri Rand*
Technion—Israel Institute of Technology, 32000 Haifa, Israel
and
Richard J. Peyran†
NASA Ames Research Center, Moffett Field, California 94035

An experimental demonstration is presented of the influence and the effectiveness of tiltrotor wing couplings in postponing whirl–flutter instability in forward flight. The experimental setup is based on a small-scale model where the wing supplies a coupled elastic support but does not introduce any aerodynamic contribution. The elastic deformation of the beam has been measured using a system of strain gauges at its root. Stability characteristics were calculated based on the recorded time history of the system response to an external abrupt disturbance. Beamwise bending–chordwise bending couplings were created by tilting the wing structure, whereas beamwise bending–twist couplings were introduced by changing the nacelle length. Both types of the wing coupling effects were found influential. The results indicate that adequate exploiting of wing coupling effects has the potential to significantly improve the stability characteristics of coupled rotor–wing systems.

Introduction

WHIRL–FLUTTER instability characteristics of wing–rotor systems are known to be important contributors to the flight envelope constraint of high-speed tiltrotors when operating in the airplane mode. This instability phenomenon is substantially different from fixed–wing aircraft flutter and is mainly derived by the coupling between the elastic wing deformation and the rotor, which is (typically) connected to the wing tip. The literature contains a wide spectrum of theoretical and experimental studies of the associated phenomena, and the references cited in what follows represent well the research effort that has been invested in understanding and controlling whirl–flutter instability phenomena over the last four decades.

The evolution and the aeromechanical characteristics of tiltrotor aircraft have been discussed in numerous reviews.[1–6] Therefore, without any attempt to thoroughly review the related research documentation, it is convenient to classify the reported studies into a few categories. References 7–11 represent the classical analyses that were aimed toward the basic understanding of the specific characteristics of whirl–flutter instability. Analytic simulations and correlations with experimental data are reported in Refs. 2 and 12–21. These models are based on a vast range of simplifying assumptions, although, in general, it may be stated that most of the effort has been devoted to the rotor system analysis and tailoring, while only relatively simple models for the wing were utilized. Flight test data are reported in Refs. 22–25, whereas Refs. 26–30 are mainly focused on hover ground tests or wind-tunnel tests of full-scale or reduced-scale rotors.

The present study is focused on the role of the wing structure and its influence on whirl–flutter instability characteristics. References 31–33 discussed the importance and impact of wing structure and wing weight on tiltrotor design. It may be shown that wing weight is primarily driven by the whirl–flutter stability safety margin (see Ref. 34). Moreover, recent studies reported in Ref. 18–20, and 35–37 have indicated that the introduction of structural couplings into the wing degrees of freedom may be exploited to postpone whirl–flutter instability. Active control methodologies that are aimed at reducing the undesired effects of the coupling between the rotor aerodynamic loads and the wing's structural dynamics for stability augmentation and vibration suppression are discussed in Refs. 38 and 39.

Because of various design requirements and constraints, currently, tiltrotor wing–rotor systems contain some structural couplings that may have a significant influence on their stability characteristics. Reference 19 discusses one specific example of beamwise bending–twist coupling that has an adverse influence on the stability of a full-scale tiltrotor configuration. Hence, the study was focused on the reduction of this coupling effect by means of introducing composite-induced beamwise bending–twist coupling into the wing structure.

Reference 37 presents the results of much more fundamental research in this direction. The study has shown that aerodynamic-induced couplings are the primary source for whirl–flutter instability and that the magnitude of these couplings is on the order of typical composite-induced couplings. The study was based on a generic composite beam model that due to its simplified geometry enabled the derivation of the involved composite-induced structural couplings in closed-form expressions and opened the way to careful examination of their effects. The results of this study have shown that the elastic couplings within the wing structure influence the aerodynamic instability effects and that using available composite materials it is possible to create strong enough elastic couplings that will reduce the amount of the overall coupling magnitude and will, therefore, contribute to the system stability.

Evidently, the literature does not contain sufficient experimental data regarding the classical whirl–flutter instability phenomena, and certainly the whole issue of wing coupling is only at its initial steps. To obtain adequate experimental data in this area, one is forced to acquire a relatively complex (and expensive) experimental setup that will be able to simulate different types of coupled wing structures.

Within the effort reported in the present paper, an experimental study has been carried out to demonstrate the feasibility of tailoring a coupled elastic wing that will substantially modify the whirl–flutter instability characteristics of the wing/rotor systems in forward flight. The experimental setup is based on a small-scale two-bladed rotor that is connected to an elastic wing structure. The wing lacks any aerodynamic fairing and, therefore, wing aerodynamics do not play any role in the present study (besides a small amount of aerodynamic

Received 9 August 1999; revision received 12 April 2000; accepted for publication 17 April 2000.

*Associate Professor, Faculty of Aerospace Engineering.
†Aerospace Engineer, Advanced Design Team, U.S. Army Aeroflightdynamics Directorate.

disturbance that is contributed by the blocking effect of the wing structure). The rotor/wing system undergoes an incoming flow, and the blade pitch angle is set to produce windmilling rotation. Thus, in the present system, there are only two sources of damping. The first source is the structural damping in the wing structure, whereas the second source is the aerodynamic damping that is provided by the rotor.

The experimental setup that has been used for the present study provides a control on the magnitude of the main two types of wing couplings, namely, the beamwise bending–chordwise bending (BB–CB) coupling and the beamwise bending–twist (BB–T) coupling. The first coupling mechanism is obtained by tilting the wing structure, whereas the BB–T coupling is obtained by adjusting the nacelle length as will be described in the next section.

It should be emphasized again that the main objective of the present study is the demonstration of the wing coupling influence on the wing-rotor system stability in forward flight. Therefore, no attempt has been made to establish consistent and adequate scaling rules (e.g., see Ref. 28) for a specific full-size configuration.

Review of Wing Coupling Effects

Before the description of the present experimental setup, the issue of wing coupling effects deserves some discussion and clarification. In general, there are a few different sources for wing couplings that should be classified to clarify the whole picture. One way to look at these wing couplings is to categorize them into the following four groups.

Loads-Induced Couplings

The coupling effects in this group are induced by some components of the loads directly or through effective arms that are created by their points or lines of application. One clear example of such effect is the coupling created by the offset between the wing shear center and the rotor hub, which may induce torsional moment when bending force is applied. Although this is a linear first-order effect, there are similar minor nonlinear effects, where due to geometry effects (elastic deformation included), certain loads may induce deformation in various directions that effectively create coupled response of the wing. The coupling effects in this group are, therefore, characterized by them all being induced as a result of loads, and, therefore, phase differences between the coupled degrees of freedom are possible. From a mathematical formulation point of view, these couplings modify the mass and the damping (in addition to the stiffness matrix) of the wing and, therefore, may be considered as dynamic couplings.

Kinematic-Induced Couplings

This category contains the structural coupling effects. The most common example of coupling in this category is the case of initially twisted wing which induce BB–CB couplings, that is, between beamwise bending and chordwise bending. Different designs may induce additional similar coupling effects that are driven by the kinematics of the structure. From a mathematical formulation point of view, kinematic induced couplings modify only the stiffness matrix of the beam and, therefore, may be considered as static couplings. In other words, the motion which is transferred from one degree of freedom to the other (coupled) degree of freedom contains no phase.

Composite-Induced Couplings

In this category, the coupling source is the fundamental coupling in the material level. Obviously, the use of composite materials does not necessarily imply that elastic couplings are introduced (see Ref. 33). However, it is well known that orthotropic composite laminas that are not balanced (namely, the material directions do not coincide with the wing axis) induce coupling between normal strain and shear stress and between shear strain and normal stress. In the structural level, these couplings may be exploited to tailor couplings between the wing transverse bending deformation components and its elastic twist. This method of introducing composite coupling effects into wing structures has been discussed and demonstrated in Refs. 19, 35, and 37. Similar to the earlier discussed kinematic-induced coupling, composite-induced couplings may be considered as static couplings.

Active-Control-Induced Couplings

In this category, which is only in its first conceptual stages as yet, active-control loads are introduced to couple certain degrees of freedom of the wing (e.g., see Ref. 38). The wing motion in this case is sensed by adequate sensors. The signals of these sensors are used to produce a command for certain actuators that may activate or modify the response of other degrees of freedom. The technology of smart structures may be adopted for introducing couplings of this type.

Experimental Setup

The experimental setup is shown in Figs. 1a and 1b and consists of a cantilever wing structure of length $l = 0.42$ m and a two-bladed rotor of a diameter $2R = 0.5$ m connected to its tip. Figure 1a shows the system setup. The wing structure may be tilted at an arbitrary angle, which determines the level of the transverse BB–CB coupling within the wing structure. In all cases, the rotor axis remains horizontal, that is, parallel to the freestream velocity. The nacelle length d, namely, the distance between the rotor hub and the wing elastic axis may also be adjusted and may, therefore, supply various BB–T couplings. The beam root region is equipped with a strain-gauge system that allows clear separation between the three main wing displacement components, namely, the beamwise bending, the edgewise bending, and the twist.

The peripheral instrumentation consists of data acquisition devices that allow simultaneous recording of the time history response of the three components of the wing deformation. Acquisition rate was set to be equal to 200 Hz, which is more than an order of magnitude higher then typical frequencies of the present wing/rotor system.

Note, again, that unlike more complex experimental procedures, the simplicity of the present experimental setup allows a wide range of parametric study that may even penetrate into the unstable region.

Wing Couplings

Figure 2 presents a scheme of the wing tip cross section, the rotor shaft, and the rotor rotation plane. As shown, the wing is tilted at an angle θ, while the shaft remains horizontal. In what follows, the vertical z direction will be denoted as the beamwise direction, whereas the horizontal y direction will be denoted as the chordwise direction. The wing structure is based on a uniform double-spar structure with three ribs (see Fig. 1a). This structure may be characterized by a uniform distribution of stiffness EI_b for bending perpendicular to the wing chord direction, EI_c for bending in the wing chord direction, and GJ for the torsional rigidity. Thus, for $\theta = 0$, no structural couplings are induced. Note that the profile-shaped ribs do not affect the characteristics.

Introducing a nonzero wing tilt angle θ modifies the described wing characteristics. When a vertical force F_z is applied at the shear center of the wing tip cross section, the tip is deflected in both y and z directions. Simple structural considerations show that this BB–CB coupling may be expressed as

$$\frac{v}{w} = \frac{\sin\theta\cos\theta[1 - (EI_b/EI_c)]}{\sin^2\theta[1 - (EI_b/EI_c)] - 1} \tag{1}$$

Similarly, when a horizontal force F_y is applied at the shear center of the wing tip cross section, the tip is deflected in both y and z directions, which constitute the following edgewise BB–CB coupling:

$$\frac{w}{v} = \frac{\sin\theta\cos\theta[1 - (EI_b/EI_c)]}{\cos^2\theta[1 - (EI_b/EI_c)] - 1} \tag{2}$$

As shown by Eqs. (1) and (2), for given values of EI_b and EI_c, the angle θ may be used to create different BB–CB couplings. In addition, also note that the region of low tilt angle θ is characterized by low effective beamwise bending stiffness and high effective

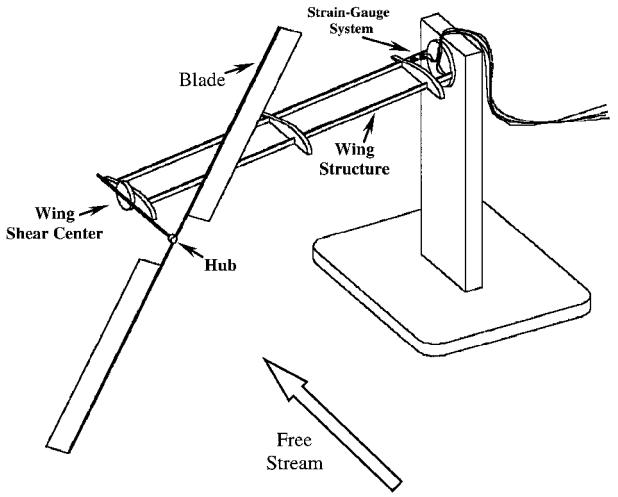

Fig. 1a General view of the experimental setup.

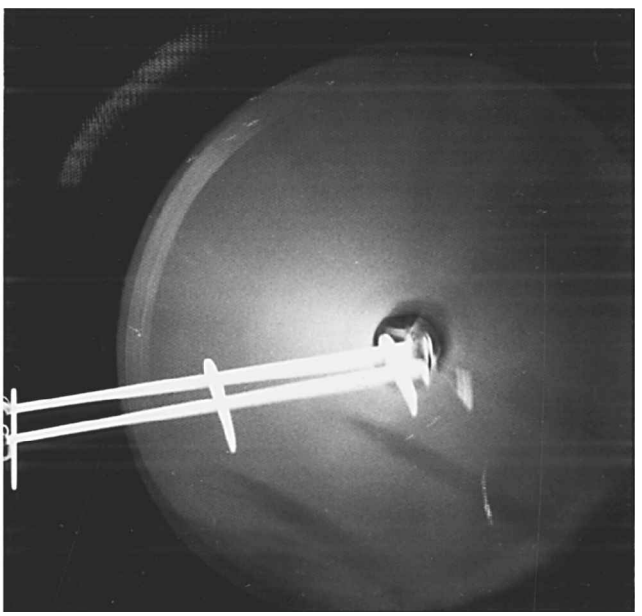

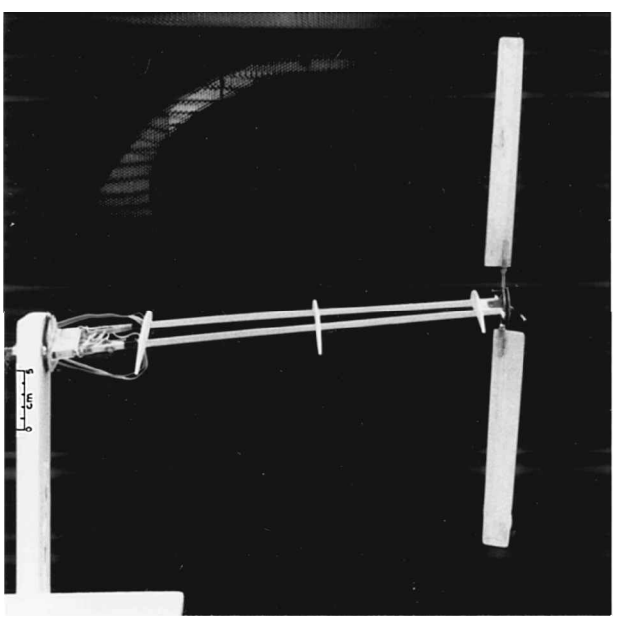

Fig. 1b Experimental setup in stationary and rotating states.

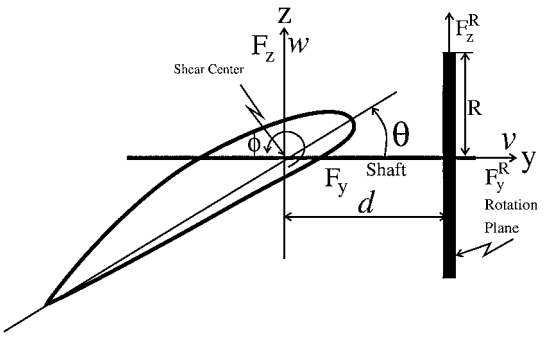

Fig. 2 Scheme of the wing tip cross section, the rotor shaft, and the rotor rotation plane.

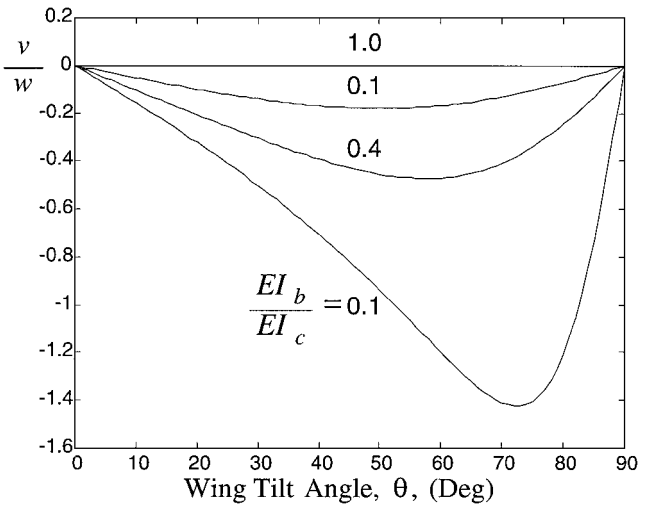

Fig. 3 Calculated wing BB–CB coupling magnitudes as a function of the wing tilt angle.

edgewise bending stiffness, whereas the region of high tilt angle is characterized by high beamwise bending stiffness and low edgewise bending stiffness.

Figure 3 presents the BB–CB coupling as a function of the wing tilt angle θ for various ratios of EI_b/EI_c. It is shown that substantially coupled wings may be obtained by the present methodology. For the actual wing structure of the experimental setup, $EI_b/EI_c = 0.42$.

Based on the notation presented in Fig. 2, the BB–T coupling, namely, the amount of twist angle that is obtained per unit beamwise deflection at the tip, may be written in the static case as

$$\frac{\Delta\phi}{w/l} = 3\left(\frac{d}{l}\right)\frac{(EI_b/GJ)}{\cos^2\theta + \sin^2\theta(EI_b/EI_c)} \tag{3}$$

As shown, the magnitude of BB–T coupling depends on the two independent parameters of this study, namely θ and d/l. The preceding expression emerges from that, on one hand, the induced moment varies linearly with the nacelle length d, but on the other hand, the bending stiffness is a function of the wing tilt angle θ. This variation is shown in Fig. 4. Similar to Fig. 3, it is shown that the present experimental methodology provides coverage of vast values of wing couplings. For the actual wing structure of the experimental setup, $EI_b/GJ = 0.95$.

For the sake of clarity, it should be emphasized that the BB–T coupling expression reflects only the static portion of this couplings, which in general may be classified as "loads-induced coupling" (see earlier discussion). This is because this coupling emerges from a beamwise force that creates a torsional moment at the wing shear center. Therefore, all force components, namely, components that are also proportional to the time derivatives of ϕ and w, should be considered. The most generic way to express this coupling is by

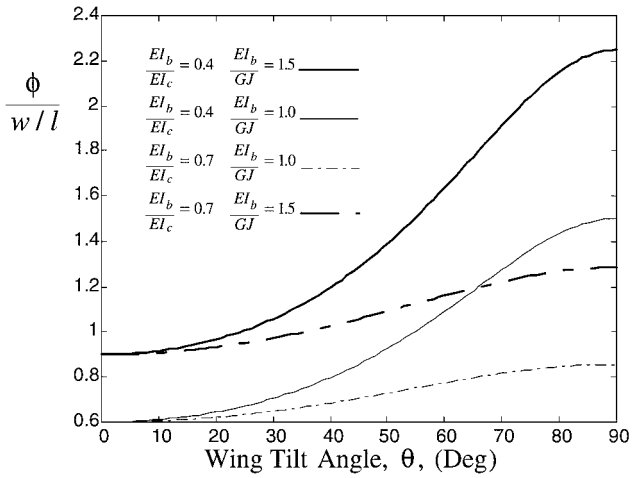

Fig. 4 Calculated wing BB–T coupling magnitudes as a function of the wing tilt angle, *d*/*R* = 0.2.

expressing the additional torsional moment that is induced by the beamwise forces ΔM as

$$\Delta M(t) = F(t) \cdot d \tag{4}$$

By taking into account the dynamics of the torsional moment and that F contains time derivatives of w, it becomes clear that $\Delta\phi$ and w may be of different phase in contrast with the v and w values that have to appear in phase in the BB–CB coupling [see Eqs. (1) and (2)].

Note that the composite-induced elastic couplings that were discussed in Refs. 19 and 37 are all inherent couplings within the wing structure and, therefore, are more comparable to the earlier discussed BB–CB couplings.

Data Reduction

Typically, the recorded time history response of the wing-rotor system consists of a transient response and a vibratory steady-state response. The transient response is due to the abrupt forcing that has been externally applied to examine the stability characteristics. The steady-state vibratory motion is a result of the imperfection of the experimental setup and mainly due to the aerodynamic disturbances that are contributed by the blocking effect of the wing structure that occurs over a thin portion of the azimuthal travel of the blades. Thus, to simplify the analysis, the vibratory time response of each one of the associated degrees of freedom may be approximated using a second-order dynamic response of a single-degree-of-freedom system, for example, $x(t)$, as

$$x(t) = x_0 e^{-\zeta\omega_0 t}\cos(\omega t - \varphi_0) + x_D\cos(\omega t - \varphi_D) \tag{5}$$

where x_0 is the transient amplitude at time zero and x_D and φ_0 are the steady-state vibratory amplitude and phase, respectively. Also, ω is the mode frequency and ζ is its damping coefficients $[\omega = \omega_0\sqrt{(1-\zeta^2)}]$. Note that, in fact, all wing modes are excited by the abrupt forcing at the tip; however, it may be shown that the first (low-frequency) modes are the most important and influential for stability analysis. This behavior will be clearly shown by the high-frequency response that is modulated on the low-frequency signature of the dominant mode.

The transient signature was analyzed using standard exponential decay analysis. Reference 40 presents a determination of the XV-15 tiltrotor configuration aeroelastic modes from flight data with frequency-domain methods and provides a discussion of the various analysis methods. In the present study, the response frequency was first estimated using fast Fourier transform technique, which has been applied to both the transient and the steady vibratory regions of the response. Once the frequency was determined, the damping coefficient was evaluated using the ratio of the response peaks at two different peak points, for example, the peak points at the end of the nth and the mth periods, namely, the times $t_n \cong 2\pi n/\omega_0 + t_0$ and $t_m \cong 2\pi m/\omega_0 + t_0$, respectively, where $m > n$ and t_0 is a constant. Based on Eq. (5), the damping coefficient in this case is estimated as

$$\zeta = [1/2\pi(m-n)]\log(x_n/x_m) \tag{6}$$

Wing Coupling Effectiveness

As already mentioned, the present study was carried out for two independent coupling parameters. The first parameter was the wing tilt angle θ that has been swept from 0 to 90 deg in steps of 15 deg, whereas the second independent parameter was the nacelle length d that has been assigned to three discrete values of $d/R = 0.19$, 0.30, and 0.42 (see Fig. 2). Three freestream velocity magnitudes were tested.

Figures 5a–5c present some typical time history responses of a relatively highly damped configuration where $\theta = 15$ deg and $d/R = 0.42$. The response is presented with a time shift that ensures that

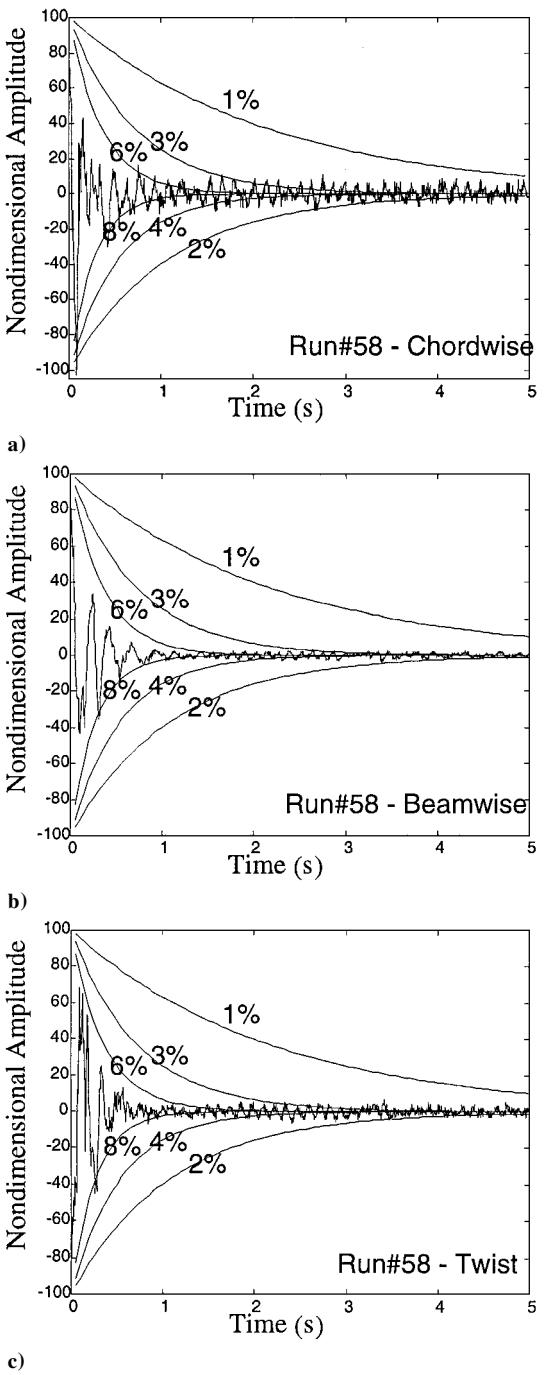

Fig. 5 Highly damped case typical signals: a) chordwise response, b) beamwise response, and c) twist response.

$t = 0$ occurs at the maximal absolute response amplitude, whereas zero amplitude is defined as the time-averaged response at the steady-state region, that is, the time average of the response after more then 5 s. All values are normalized and presented as percents of the already given maximal absolute response amplitude. In addition to the experimental signals, Figs. 5a–5c also contain calculated envelopes of decay for various damping coefficient. Even without the described formal estimation of the damping, it is clear that in this sample response the damping ratio is about 8%.

For obvious reasons, operation of the experimental setup in unstable vibratory region for extended periods has been avoided. However, because of the relatively low amount of energy that is stored in the present experimental model, safety margins were reached only for cases that were very close to instability. For illustration, Fig. 6 presents one case of very low, virtually zero, damping, where it is evident that the response envelope consists of horizontal lines.

Figures 7a–7c present the wing damping as a function its tilt angle for the three values of forward flight velocity. As shown in the case of $V = 2.3$ m/s (see Fig. 7a), a clear trend of decreasing damping for increasing values of θ is observed for the low nacelle lengths, whereas for the case of high nacelle length, the damping recovers for high values of θ. The results, therefore, indicate that the BB–CB coupling has an adverse effect on stability, and in general, the BB–T coupling has a similar effect. For the case of $V = 3.5$ m/s (see Fig. 7b), the BB–T coupling has a negative effect, whereas the BB–CB coupling has a positive effect at high values of θ. For the case of $V = 4.6$ m/s (see Fig. 7c), in general, the BB–T coupling has a negative effect, whereas the BB–CB coupling effect has an adverse effect as well, and in fact, all cases above $\theta = 45$ deg are unstable.

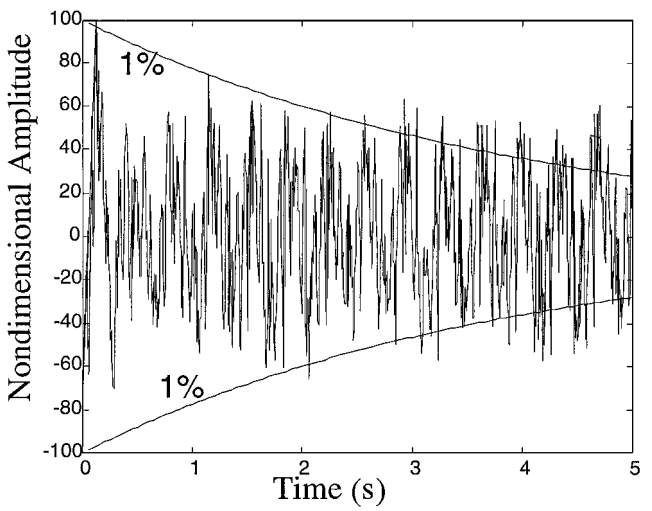

Fig. 6 Beamwise bending signal of an undamped case.

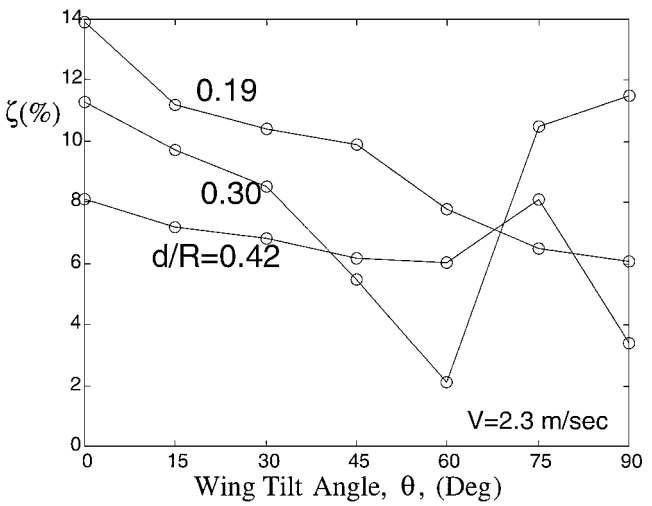

Fig. 7a Wing damping as a function of the wing tilt angle for low forward flight velocity.

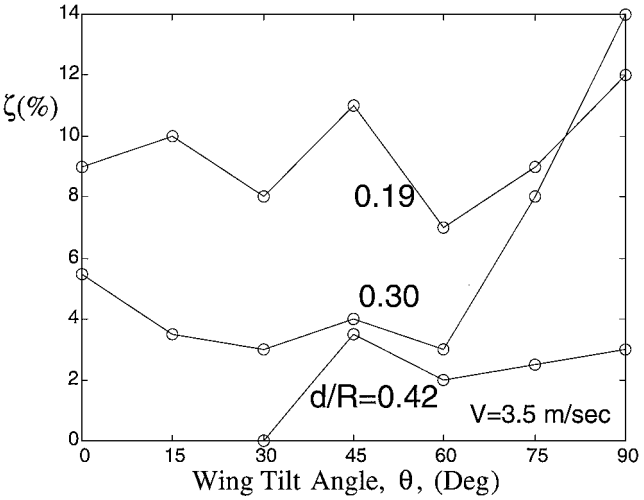

Fig. 7b Wing damping as a function of the wing tilt angle for medium forward flight velocity.

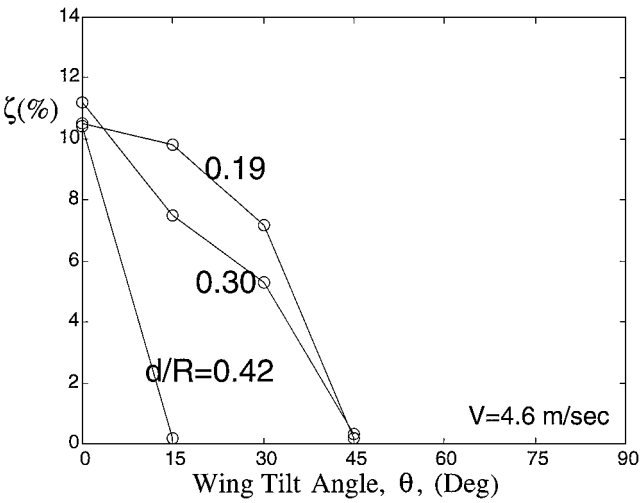

Fig. 7c Wing damping as a function of the wing tilt angle for high forward flight velocity.

Therefore, it is clear that elastic couplings (which may be achieved by a wide range of different means) are highly influential. A clear representative point is the case of $\theta = 15$ deg at $V = 4.6$ m/s (Fig. 7c). As shown, increasing the BB–T coupling from the case of $d/R = 0.19$ to the case of $d/R = 0.42$ results in the damping decreasing from 10 to 0%. According to Fig. 4 and Eq. (3), the corresponding BB–T coupling values in this case are $\phi l/(w) = 0.65$ for $d/R = 0.19$ and $\phi l/(w) = 1.4$ for $d/R = 0.42$. This finding coincides with the results of Ref. 19, where composite-induced couplings were used to lessen the instability contributed by similar BB–T coupling effects.

Conclusions

An experimental methodology for studying the influence of wing couplings on the stability characteristics of wing-rotor systems has been offered. Mainly, it is suggested to introduce elastic couplings by tilting the wing structure and varying the nacelle lengths.

The study described is based on a small-scale model of a wing-rotor system. Thus, in light of the well known difficulties to scale correctly the structural dynamics and the effective aeroelastic properties, the present analysis serves only as a demonstrator for the associated phenomena. However, it is expected that the present simple experimental methodology will also serve as a reference for correlating analytic models that feature wing structural elastic couplings.

Such a correlation may contribute to the prediction quality of full-scale configurations as well.

In general, wing couplings were found to be very influential. It may be concluded that wing couplings may be exploited in two different ways. First, because currently various design constraints lead to tiltrotor configurations that include couplings of adverse influence, introducing additional opposite couplings may lessen these effects significantly and contribute to the stability characteristics of the entire wing-rotor system. Second, in light of the discussed possibilities to tailor the wing structure of new designs in various manners, the present results contribute additional evidence of the potential of this method to augment wing–rotor stability in forward flight.

References

[1]Anderson, S. B., "Historical Overview of V/STOL Aircraft Technology," NASA TM 81280, March 1981.

[2]Johnson, W., Lau, B. H., and Bowles, J. V., "Calculated Performance, Stability and Maneuverability of High-Speed Tilting-Prop-Rotor," NASA TM 88349, Sept. 1986.

[3]Felker, F. F., "A Review of Tilt Rotor Download Research," *14th European Rotorcraft Forum*, Milano, Italy, Sept. 1988, pp. 14.1–14.31.

[4]Fradenburgh, E. A., "High Speed Challenge for Rotary Wing Aircraft," *International Pacific Air and Space Technology Conference and 29th Aircraft Symposium Proceedings*, Gifu, Japan, Oct. 1991, pp. 91–109.

[5]Kvaternik, R. G., "A Historical Overview of Tiltrotor Aeroelastic Research at Langley Research Center," NASA TM 107578, April 1992.

[6]Lynn, R. R., "The Rebirth of the Tiltrotor—The 1992 Alexander A. Nikolsky Lecture," *Journal of the American Helicopter Society*, Vol. 38, No. 1, 1993, pp. 3–16.

[7]Houbolt, J. C., and Reed, W. H., "Propeller–Nacelle Whirl Flutter," *Journal of the Earospace Sciences*, Vol. 29, No. 3, March 1962, pp. 333–346.

[8]Hall, W. E., "Prop–Rotor Stability at High Advance Ratios," *Journal of the American Helicopter Society*, Vol. 11, No. 2, 1966, pp. 11–26.

[9]Reed, W. H., "Review of Propeller-Rotor Whirl Flutter," NASA TR R-264, July 1967.

[10]Young, M. T., and Lytwyn, R. T., "The Influence of Blade Flapping Restraint on the Dynamic Stability of Low Disk Loading Propeller-Rotor," *23th Annual Forum of the American Helicopter Society*, Washington, DC, May 1967, pp. 38–54.

[11]Edenborough, H. K., "Investigation of Tilt-Rotor VTOL Aircraft Rotor-Pylon Stability," *Journal of Aircraft*, Vol. 5, No. 6, 1968, pp. 97–105.

[12]Johnson, W., "Theory and Comparison With Tests of Two Full-Scale Proprotors," *AHS/NASA-Ames Specialists' Meeting on Rotorcraft Dynamics*, California, USA, 13–15 Feb. 1974, pp. 1–11.

[13]Johnson, W., "Dynamics of Tilting Proprotor Aircraft in Cruise Flight," NASA TN D-7677, May 1974.

[14]Johnson, W., "Analytical Modeling Requirements for Tilting Proprotor Aircraft Dynamics," NASA TN D-8013, July 1975.

[15]Johnson, W., "An Assessment of the Capability to Calculate Tilting Prop-Rotor Aircraft Performance, Loads, and Stability," NASA TP–2291, March 1984.

[16]Totah, J. J., "Description of a Tilt Wing Mathematical Model for Piloted Simulation," *47th Annual Forum of the American Helicopter Society*, Phoenix, AZ, May 1991, p. 16.

[17]Moore, M. J., Yablonski, M. J., Mathew, B., and Liu, J., "High Speed Tiltrotors: Dynamics Methodology," *49th Annual Forum of the American Helicopter Society*, St. Louis, MO, May 1993, pp. 1255–1268.

[18]Nixon, M. W., "Parametric Studies for Tiltrotor Aeroelastic Stability in Highspeed Flight," *Journal of the American Helicopter Society*, Vol. 38, No. 4, 1993, pp. 71–79.

[19]Popelka, D., Lindsay, D., Parham, T., Berry, V., and Baker, D. J., "Results of an Aeroelastic Tailoring Study for a Composite Tiltrotor Wing," *Journal of the American Helicopter Society*, Vol. 42, No. 2, 1997, pp. 126–136.

[20]Corso, L. M., Popelka, D. A., and Nixon, M. W., "Design, Analysis, and Test of a Composite Tailored Tiltrotor Wing," *53rd Annual Forum of the American Helicopter Society*, Virginia Beach, VA, April–May 1997, pp. 209–219.

[21]Srinivas, V., and Chopra, I., "Validation of a Comprehensive Aeroelastic Analysis for Tiltrotor Aircraft," *Journal of the American Helicopter Society*, Vol. 43, No. 4, 1998, pp. 333–341.

[22]Schroers, L. G., "Dynamic Structural Aeroelastic Stability Testing of the XV-15 Tilt Rotor Research Aircraft," NASA TM-84293, Dec. 1982.

[23]Arrington, W. L., Kumpel, M., Marr, R. L., and McEntire, W. G., "XV-15 Tilt Rotor Research Aircraft Flight Test Data Report, Volume II: Performance and Handling Qualities," NASA CR-NAS2-7600, June 1985.

[24]Arrington, W. L., Kumpel, M., Marr, R. L., and McEntire, K. G., "XV-15 Tilt Rotor Research Aircraft Flight Test Data Report, Vol III: Structural Loads and Dynamics," NASA CR 177406, U.S. Army Aviation Systems Command, TR-86-A-1, June 1985.

[25]Brunken, J. E., Popelka, D. A., and Bryson, R. J., "A Review of the V-22 Dynamics Validation Program," *45th Annual Forum of the American Helicopter Society*, Boston, MA, May 1989, pp. 51–63.

[26]Alexander, H. R., Hengen, L. M., and Weiberg, J. A., "Aeroelastic-Stability Characteristics of a V/STOL Tilt-Rotor Aircraft with Hingeless Blades: Correlation of Analysis and Test," *30th Annual Forum of the American Helicopter Society*, Washington, DC, May 1974, pp. 12–22.

[27]Bartie, K., Alexander, H., McVeigh, M., La Mon, S., and Bishop, H., "Hover Performance Test of Baseline Metal and Advenced Technology Blade (ATB) Rotor System for the XV-15 Tilt Rotor Aircraft," NASA CR 177436, Contract NAS2-11250, Oct. 1986.

[28]Settle, T. B., and Kidd, D. L., "Evolution and Test History of the V-22 0.2-Scale Aeroelastic Model," *Journal of the American Helicopter Society*, Vol. 37, No. 1, Jan. 1992, pp. 31–45.

[29]Light, J. S., "Results from An XV-15 Rotor Test in the National Full-Scale Aerodynamics Complex," *53th Annual Forum of the American Helicopter Society*, Virginia Beach, VA, May 1997, pp. 231–239.

[30]Light, J. S., Kitaplioglu, C., and Acree, C. W., "XV-15 Aeroacoustic Testing at NASA Ames," *23th European Rotorcraft Forum*, Dresden, Germany, Sept. 1997, pp. 109.1–109.10.

[31]Chappell, D. P., and Peyran, R. J., "Methodology for Estimating Wing Weights for Conceptual Tilt-Rotor and Tilt-Wing Aircraft," 51st Annual Conf. of the Society of Allied Weight Engineers, Inc., Hartford, CT, 18–20 May 1992, pp. 1–12.

[32]Sprangers, C. A., and Stevenson, M. K., "Results of the V-22 Preliminary Design Wing Test Program," 42nd Annual Forum of the American Helicopter Society, Washington, DC, June 1986, pp. 327–338.

[33]Senn, E. E., "The Effects of Composite Material on the Configuration and Design of the V-22 Wing," American Helicopter Society National Technical Specialists' Meeting on Rotorcraft Structures, Williamsburg, VA, Oct. 1991, pp. 1–6.

[34]Peyran, R., and Rand, O., "The Effect of Design Requirements on Conceptual Tiltrotor Wing Weight," 55th Annual Forum of the American Helicopter Society, Montreal, Quebec, Canada, Aircraft Design I/4, May 1999.

[35]Lake, R. C., Nixon, M. W., and Wilbur, M. L., "Demonstration of an Elastically Coupled Twist Control Concept for Tilt Rotor Blade Application," *AIAA Journal*, Vol. 32, No. 7, 1994, pp. 1549–1551.

[36]Kosmatka, J. B., and Lake, R. C., "Passive Approach of Controlling Twist in Composite Tilt-Rotor Blades," *SPIE Conference on Smart Structures and Integreted Systems*, San Diego, CA, 26–29 Feb. 1996, pp. 146–157.

[37]Barkai, S. M., and Rand, O., "The Influence of Composite Induced Couplings on Tiltrotor Whirl Flutter Stability in Forward Flight," *Journal of the American Helicopter Society*, Vol. 44, No. 2, 1998, pp. 133–145.

[38]Van Aken, J. M., "Alleviation of Whirl-Flutter on Tilt-Rotor Aircraft Using Active Controls," *47th Annual Forum of the American Helicopter Society*, Phoenix, AZ, May 1991, pp. 1321–1344.

[39]Settle, T. B., and Nixon, M. W., "MAVSS Control of an Active Flaperon for Tiltrotor Vibration Reduction," *53rd Annual Forum of the American Helicopter Society*, Virginia Beach, VA, April–May 1997 pp. 1–17.

[40]Acree, C. W., and Tischler, M. B., "Determining XV-15 Aeroelastic Modes from Flight Data with Frequency-Domain Methods," NASA TP 3330, U.S. Army Aviation and Troop Command, TR 93-A-004, May 1993.